Lidar-Measured Winds from Space: A Key Component for Weather and Climate Prediction

Wayman E. Baker,* George D. Emmitt,+ Franklin Robertson,# Robert M. Atlas,@ John E. Molinari,& David A. Bowdle,** Jan Paegle,++ R. Michael Hardesty,## Robert T. Menzies,@@ T. N. Krishnamurti,&& Robert A. Brown,*** Madison J. Post,## John R. Anderson,+++ Andrew C. Lorenc,### and James McElroy@@@

Abstract

The deployment of a space-based Doppler lidar would provide information that is fundamental to advancing the understanding and prediction of weather and climate.

This paper reviews the concepts of wind measurement by Doppler lidar, highlights the results of some observing system simulation experiments with lidar winds, and discusses the important advances in earth system science anticipated with lidar winds.

Observing system simulation experiments, conducted using two different general circulation models, have shown 1) that there is a significant improvement in the forecast accuracy over the Southern Hemisphere and tropical oceans resulting from the assimilation of simulated satellite wind data, and 2) that wind data are significantly more effective than temperature or moisture data in controlling analysis error. Because accurate wind observations are currently almost entirely unavailable for the vast majority of tropical cyclones worldwide, lidar winds have the potential to substantially improve tropical cyclone forecasts. Similarly, to improve water vapor flux divergence calculations, a direct measure of the ageostrophic wind is needed since the present level of uncertainty cannot be reduced with better temperature and moisture soundings alone.

*National Centers for Environmental Prediction, Camp Springs, Maryland.
+Simpson Weather Associates, Charlottesville, Virginia.
#NASA/Marshall Space Flight Center, Huntsville, Alabama.
@NASA/Goddard Space Flight Center, Greenbelt, Maryland.
&State University of New York at Albany, Albany, New York.
**University of Alabama at Huntsville, Huntsville, Alabama.
++University of Utah, Salt Lake City, Utah.
##NOAA/Environmental Technology Laboratory, Boulder, Colorado.
@@NASA/Jet Propulsion Laboratory, Pasadena, California.
&&The Florida State University, Tallahassee, Florida.
***University of Washington, Seattle, Washington.
+++Space Science and Engineering Center, Madison, Wisconsin.
###United Kingdom Meteorological Office, Bracknell, United Kingdom.
@@@Environmental Protection Agency, Las Vegas, Nevada.
Corresponding author address: Dr. Wayman E. Baker, National Centers for Environmental Prediction, 5200 Auth Road, Camp Springs, MD 20746.
In final form 19 December 1994.

1. Introduction

Knowledge of the global wind field is widely recognized as fundamental to advancing the understanding and prediction of weather and climate. Studies have concluded that it is possible to measure tropospheric winds from space with current lidar technology (Huffaker 1978; Huffaker et al. 1980; Huffaker et al. 1984; Menzies 1986; NASA 1979, 1982, 1987). In addition, successful experimental demonstrations of a 5 J-class, CO_2 laser were conducted in the laboratory as part of the design studies for the Laser Atmospheric Wind Sounder (LAWS) instrument (General Electric Astro Space 1992; Lockheed 1992). Because of the extended airborne and ground-based heritage of the CO_2 Doppler wind lidar (demonstrated accurate wind measurement capability since 1968) and the strong potential for advances in earth system science, the LAWS instrument was recommended in 1985 for inclusion in the National Aeronautics and Space Administration (NASA) Earth Observing System (EOS) instrument suite.

Budgetary pressure on the EOS program was a key factor in the deselection of the LAWS instrument and science team from EOS in early 1994. The former science team continues to meet as the National Oceanic and Atmospheric Administration (NOAA) Working Group on Space-Based Lidar Winds. The working group and personnel at the NASA/Marshall Space Flight Center are focusing on an instrument concept and science objectives for a small-satellite version of LAWS. The recent advances with the 2-μm solid-state lidar (Henderson et al. 1993) make that technology competitive for such a mission. However, this paper focuses on the original LAWS concept (i.e., with a 20 J CO_2 laser), which is well understood and remains a long-term goal of the authors. The mission measurement requirements and possible parameters are summarized in Table 1.

TABLE 1. Measurement requirements and possible parameters for a full-capability wind lidar mission.

Mission requirements	Possible mission parameters
Accuracy (vector wind)	**Orbit**
2 m s^{-1}, 0–3 km	525 km
3 m s^{-1}, 3–15 km	98° inclination
	(sun synchronous)
Resolution	**Lidar**
Horizontal—1 wind vector	~20 J CO_2 laser
per 100-km box	~1.5-m telescope
Vertical—0.5 km from 0–2 km	5-Hz average sampling rate
1 km from 2–15 km	20-Hz peak sampling rate
Temporal—Every 12 hours	2–3-μs pulse
(6 hours desired)	
Coverage	**Scan**
Horizontal—global	10–15 rpm
Vertical—0–15 km	Conical
	40°–50° nadir angle

It is acknowledged that the measurement of winds in the "clear" upper troposphere is challenging and that other techniques such as direct detection (Abreu et al. 1992; Korb et al. 1992) and the use of shorter wavelength solid state transmitters may offer some potential advantages in sampling the lower troposphere. However, at this time coherent CO_2 systems remain the most mature technology for space-based measurement of tropospheric winds.

This paper discusses the concept of a space-based Doppler lidar and the expected scientific return with its measurements. Specifically, in section 2, the measurement concepts for a Doppler wind lidar are reviewed. The results of some Observing System Simulation Experiments (OSSEs) with lidar winds are discussed in section 3. In section 4 the anticipated advances in earth system science with lidar winds are highlighted. Finally, some concluding remarks are made in section 5.

2. Doppler lidar wind measurement concepts

a. General principles

The basic concepts associated with the application of coherent Doppler lidar for wind measurements are discussed by Menzies and Hardesty (1989). A Doppler lidar, such as the one envisioned for LAWS, operates much like Doppler radar in that signals returned to the receiver from distant targets are spectrally analyzed to recover the Doppler shifts imposed by the motion of the target. The short wavelengths (e.g., ~9 μm) involved in lidar, however, mean that the targets can be much smaller than for radar and that comparative Doppler shifts and signal bandwidths are much greater. The distributed nature of the backscatter material means that a pulse of light transmitted from the lidar (see Fig. 1) gives rise to a return signal that is scattered as it propagates through the atmosphere and is finally reflected from the earth's surface. Range resolution is obtained by dividing the return signal into sequential time intervals, referred to as range gating. For wind sensors, the targets are cloud particles or naturally occurring aerosols suspended in the atmosphere, which move at approximately the speed of the wind. An objective of the upcoming Multicenter Airborne Coherent Atmospheric Wind Sensor mission in 1995 (J. Rothermel 1994, personal communication) is to assess how accurately the motion of the aggregate of cloud particles represents the environmental wind.

An orbiting Doppler lidar (see cover illustration) consists of a reasonably high-energy, pulsed single-frequency laser, a meter-size telescope, which acts as an optical antenna (analogous to radar), with a heterodyne detector in the focal plane. The detected heterodyne signal resides in the radio frequency domain and is Doppler shifted due to the motion of the spacecraft and the line-of-sight (LOS) component of the wind. The telescope scans about nadir as the spacecraft proceeds along its orbit tracing a spiral pattern centered about the ground track. The different perspectives afforded by the scanning geometry enable the horizontal wind vectors to be recovered.

The application of Doppler lidar for the measurement of winds has been extensively demonstrated

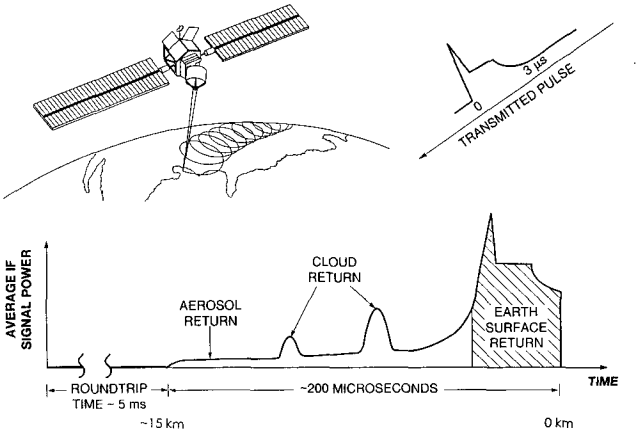

FIG. 1. Principles of Doppler lidar.

from both airborne and ground-based platforms. For airborne applications, a low-energy system was used to study winds in the vicinity of severe storms and other dynamic processes during the 1970s and early 1980s (Bilbro and Vaughan 1978; Bilbro et al. 1986; Emmitt 1985a,b). In 1986, scientists at NOAA demonstrated a ground-based pulsed system that was conceptually very similar to the LAWS system, albeit with reduced pulse energy and telescope size (Hardesty et al. 1988). The NOAA system has been employed extensively to study a variety of atmospheric phenomena, including thunderstorm outflows (Intrieri et al. 1990), upper-level winds associated with a strong frontal passage (Neiman et al. 1988), and sea-breeze evolution (Banta et al. 1993). Because the sensitivity of the NOAA system has been well documented (e.g., Post and Cupp 1990), results from the NOAA field studies can be extrapolated to predict the performance of a space-based lidar system.

In addition, solid-state and CO_2 airborne-pulsed Doppler lidar systems have been demonstrated in forward- and side-looking modes with fixed pointing. An airborne CO_2-pulsed Doppler lidar system has been demonstrated in a side-looking mode with coplanar scanning and fore/aft velocity components for vector velocity resolution (Bilbro and Vaughan 1978; Bilbro et al. 1984; Bilbro et al. 1986); a second-generation system will fly in 1995 (J. Rothermel 1994, personal communication). Also, a downward-looking conically scanning airborne-pulsed CO_2 Doppler lidar (Werner et al. 1989) is scheduled for first flight in 1996 (J. Rothermel 1994, personal communication).

b. Global aerosol backscatter distributions

Although an earth-orbiting Doppler lidar would be programmed to probe the atmosphere with $(2.5–3.0) \times 10^4$ shots per orbit, not all the shots would reach the earth's surface or return a signal of sufficient strength to make an LOS wind measurement. Thirty to forty percent of the shots would be terminated by thick clouds before reaching the ground, with LOS winds produced at those levels. An additional 30%–50% of the time, thin or semitransparent clouds would also provide a strong return but would allow for observations further along the LOS (Emmitt and Séze 1991). In all other cases, aerosols, depending on their size and concentration, would have to provide the backscatter necessary for good LOS measurements.

Values of the volume backscatter coefficient β (m^{-1} sr^{-1}) for atmospheric aerosols and clouds can easily range over six to eight orders of magnitude (Kent et al. 1983a; Kent et al. 1983b; Yue et al. 1983; Hall et al. 1988) depending on the wavelength. During the early conceptual studies on the precursor to LAWS, referred to as WINDSAT (wind satellite) (Huffaker 1978; Huffaker et al. 1980; Huffaker et al. 1984), very little information was available on atmospheric backscatter properties at or near the prospective LAWS wavelength of 9.11 μm. In fact, Huffaker et al. (1984) identified uncertainties in aerosol backscatter properties as the largest single uncertainty in their WINDSAT feasibility study.

In recognition of this critical data gap, NASA and NOAA supported three workshops on infrared backscatter for aerosols between 1983–85, and in 1986 NASA initiated the Global Backscatter Experiment (GLOBE) as a cooperative interagency and international effort to document global aerosol backscatter distributions for input to LAWS development studies (Bowdle 1986, 1989). This research effort has been directed toward modeling the spatial, temporal, and spectral variations of aerosol backscatter coefficients in the troposphere and lower stratosphere. The study has emphasized aerosol backscatter properties at selected CO_2 laser wavelengths, initially 10.6 μm, building on the NOAA dataset (Post 1984a; Bowdle et al. 1991), and later 9.25 μm, beginning with the Jet Propulsion Laboratory dataset (Ancellet et al. 1988; Menzies et al. 1989). However, from its inception, the program has also provided measurement and modeling of aerosol backscatter at shorter wavelengths to support studies on solid-state 2.1-μm wavelength alternatives to the CO_2 gas laser. Similarly, GLOBE has emphasized backscatter properties over the remote oceans and in the middle and upper troposphere. These are the regions where lidar wind measurements are most needed for assimilation into general circulation models. GLOBE research efforts have also included studies of clouds, marine aerosols, and other high-backscatter targets for use in studies of smaller lidar prototypes.

Several papers relevant to GLOBE findings were published in a special GLOBE section of the March 1991 *Journal of Geophysical Research—Atmospheres.* Results since that time have confirmed the presence of a well-defined multimodal frequency distribution of aerosol backscatter values (see Fig. 4). The primary mode, which appears to account for 40%–50% of all tropospheric backscatter, is the so-called "background" mode in the middle and upper troposphere (Rothermel et al. 1989; Bowdle et al. 1993). This feature is characterized by low backscatter values (i.e., 10^{-11} to 10^{-10} m^{-1} sr^{-1} at CO_2 wavelengths) and, considering the large dynamic range in the rest of the atmospheric backscatter distribution, has surprisingly weak spatial/temporal variability. A slightly broader secondary mode, which accounts for ~10%–20% of the troposphere, is associated with much higher backscatter in the planetary boundary layer (PBL). Together these ubiquitous quasi–steady-

state and reasonably predictable features account for more than 60% of the tropospheric backscatter. The remaining backscatter is associated with two much-broader distributions from less predictable stochastic targets, namely water or ice clouds, and PBL aerosols that are detrained into and diluted by the background middle and upper troposphere. The diluted PBL mode (termed the "convective mode" by Rothermel et al. 1989) lies in the intermodal gap between the PBL and the background distributions. The cloud mode roughly overlaps the convective mode, although the cloud backscatter at CO_2 laser wavelengths extends about two orders of magnitude higher than the PBL mode (Menzies and Tratt 1993).

Other aerosol studies show that these general characteristics can be modified significantly by massive but transient aerosol generation events that would potentially provide significantly more wind data than would otherwise be expected. For example, in the springtime Northern Hemisphere, vigorous convection, strong zonal winds, and desert dust storms overwhelm the background mode and produce broad areas of strong backscatter (Kent et al. 1991). In addition, extremely cold temperatures inside the wintertime polar vortex produce deep and widespread polar stratospheric clouds (McCormick et al. 1982; Steele et al. 1983). Finally, major volcanic eruptions dramatically increase backscatter in the lower stratosphere for several years (Post 1984b). The troposphere tends to recover much more rapidly from these eruptions, except in the vicinity of tropopause folds, which cause mixing of lower stratospheric aerosols into the middle and upper troposphere (Kent et al. 1991; Post 1986). During extended intervolcanic periods, backscatter values in the lower stratosphere eventually decay toward values similar to those in the background in the middle and upper troposphere (Rothermel et al. 1989; Post and Cupp 1992).

c. Sampling volume

As the laser pulse propagates through the atmosphere, photons are scattered back to the lidar system. For the 20 J system, the signal on the detector is the integrated return from a cylindrical volume that is approximately 10–20 m in diameter and 300 m long. The signal is digitized at a rate of 50 Mhz and processed to provide a single estimate of the LOS Doppler shift for each 250–350-m range gate. While this may be the resolution for returns from bright targets (clouds, ground, etc.), it is more likely that several of these range gates would be processed together to provide a reliable estimate over 1–3 km, depending upon the intensity of the returns.

As mentioned earlier, the lidar beam would be scanned with a rotating mirror resulting in the cycloidal pattern of samples. A target volume of $100 \times 100 \times 1$ km^3 has been chosen in this paper to express many of the performance statistics. Given the orbit and system parameters listed in Table 1, the resulting sample density is 24 independent LOS wind measurements per target volume (four range gates per vertical kilometer times six shots per 100×100 km^2 area).

SAT. ALT.: 525 KM	INC. ANG.: 98 DEG
NADIR SCAN ANG.: 45 DEG	ENERGY: 20 J
WAVELENGTH: 9.11	TEL. DIA.: 1.5 M
FIXED AREA: 125 KM	PRF: 4.6 HZ

FIG. 2. Simulated wind observations from a 20 J LAWS for a 24-h period at 850 mb. Inputs to lidar wind simulation model were from the European Centre for Medium-Range Weather Forecasts nature run. Cloud obscurations are the primary causes of the data voids within the instrument-viewing swath.

d. Sampling strategies and shot management

To extend the lifetime of the laser, shot management involving reduced high latitude (polar) sampling has been proposed. As may be seen in Fig. 2, the orbital swaths overlap poleward of 45°. A shot management algorithm designed to achieve the same 12-h sampling interval for the Tropics as for the poles would reduce the total shots per orbit by 25%–30% without compromising global coverage.

Another possible consideration for laser shot management is the desire to take more samples where the ageostrophic component of the wind is predominant and/or most variable, such as in the Tropics (Houston and Emmitt 1987) and near the subtropical and polar jets.

e. Signal processing and measurement quality

Because the signal backscattered from atmospheric aerosol particles would, in many instances, be quite weak, advanced signal processing would be a critical component of a Doppler lidar instrument. When the

initial feasibility studies for a space-based lidar system were performed, a representative minimum backscatter level of 10^{-10} m^{-1} sr^{-1} was assumed (Huffaker 1978). As indicated previously, aerosol backscatter coefficients can approach background levels (~3–5 10^{-11} m^{-1} sr^{-1}) in the middle and upper troposphere over much of the globe. Thus, a Doppler lidar system will have to operate at a signal-to-noise ratio (SNR) that may be at least an order of magnitude less than originally assumed. Although some of the signal loss can be made up by increasing the laser power and telescope diameter, the challenge lies in developing signal processing and analysis techniques that can accurately estimate wind velocities at the very low SNRs encountered in these "clean" regions. The signal processing and analysis function for a Doppler lidar can be broken down into three critical tasks:

1) processing the signals backscattered from the individual laser pulses to estimate the LOS component of the wind,
2) performing some form of quality check to determine if the estimated value of the LOS component has sufficiently small error to be used in the calculation of the horizontal wind, which is especially critical when SNR is low (Rye and Hardesty 1993), and
3) combining the LOS estimates from a given area to compute a representative horizontal wind vector (Emmitt and Bilbro 1987; Emmitt 1987).

Because the instrument platform will be moving through space with a ground speed of more than 7 km s^{-1}, removal of the Doppler shift imparted to the signal by spacecraft motion is necessary for accurate estimates of the LOS wind velocity component. The telescope-pointing direction and satellite speed, measured onboard the spacecraft at the time of laser pulse transmission, will be used to compute the Doppler shift due to satellite motion. The current design calls for this frequency shift to be removed electronically; the backscattered signal will be mixed with a signal from a reference oscillator that has a frequency approximately equal to the Doppler shift imparted by the satellite motion.

The LOS velocity estimate will be computed from the information within each range gate of a single lidar return. To reduce the probability of a poor estimate at low SNR levels, it is anticipated that some form of a priori information (e.g., numerical model prediction, climatology, high confidence estimates from adjacent gates) can be used to narrow the range of potentially measurable horizontal wind speeds for each gate to ±25 m s^{-1} around a predicted value. Even with this velocity estimate "windowing," a sophisticated velocity estimation algorithm is required to optimize performance. Development of optimal estimation algorithms is an important aspect of the prelaunch effort. For LAWS system design studies, a Capon-type algorithm (Capon 1969; Marple 1987) has been assumed for the LOS velocity estimation problem; the actual LOS estimation algorithm will probably not differ substantially in performance from a tuned Capon algorithm. Simulations performed using a 20 J laser indicate that in low backscatter regimes (about 3×10^{-11} m^{-1} sr^{-1}), these estimators should be able to extract good returns from a single shot approximately 50% of the time (Emmitt 1993). Algorithm performance rises rapidly with SNR; the probability of a good single-shot estimate increases to above 95% for backscatter levels of 10^{-10} m^{-1} sr^{-1}.

The error distribution of low SNR velocity estimates consists of a narrow spike of observations at the correct velocity in a background of essentially random measurements. This highly non-Gaussian error distribution has important implications for the use of lidar winds in low SNR regions. For example, it is not appropriate to merely average the estimates from a particular spatial box. The anticipated results of such an averaging are worse than simply choosing one observation at random. To handle such cases, robust statistical techniques are being employed, such as *N* of *M* processors, where one searches for a cluster of *N* measurements that lie within a specified error tolerance from the total sample of *M* observations (often referred to as consensus averaging).

Processors of this type can be constructed with a variable spatial resolution (i.e., the size of the spatial integration box can be dynamically expanded where necessary so that estimates with lower spatial resolution can be calculated in regions of marginal SNR). For some applications it is expected that using LOS estimates directly in models will produce superior results. For these cases, care must be taken to handle the error distribution with either robust assimilation techniques or use of appropriate data quality control methods that are designed to minimize measurement biases.

In assessing the quality of lidar data, both the accuracy of the LOS measurement and its representativeness must be considered. The measurement accuracy is expressed in terms of the standard deviation (σ_m) of the lidar wind speed from the true wind components along the LOS. The representativeness of the measurements is related to the rms differences (σ_s) between the local wind along the individual LOS and the average of all possible LOS observations having the same perspective within the target volume. Differences are due to the variance of the real wind field within the target volume. Therefore, the total

variance (σ_o^2) of the error in the wind observation can be expressed as

$$\sigma_o^2 = \frac{\sigma_m^2 + \sigma_s^2}{PN}, \qquad (3.1)$$

where

- σ_m^2 is the variance in the LOS measurement due to lidar system noise, atmospheric turbulence within the sample volume, stability of the wind estimation algorithm, etc.;
- σ_s^2 is the variance of the true wind component on scales between 1 and 200 km (assuming a target volume of 100 × 100 × 1 km^3);
- σ_o^2 is the total variance between the observed components and the true average wind components within the target volume;
- N is the number of attempted LOS observations; and
- P is the fraction of N attempts that return a "good" LOS estimate.

In Eq. (3.1), both σ_m^2 and P are, in part, functions of the energy of the laser pulse. While independent of the laser energy, σ_s^2 can have its contribution to σ_o^2 reduced only by increasing PN.

Assuming a fixed and limiting platform power supply, trade studies must be conducted to minimize σ_s^2. Since the power demand of the lidar system is related to the product of the pulse repetition frequency (prf) and the energy per pulse, one important trade is between these two parameters (Emmitt and Wood 1991). For instance, high energy per pulse at a low prf achieves the best individual LOS measurements ($P \sim 100\%$) due to maximized SNR. However, since N, in this case, is very low and σ_s (≈ 3 m s^{-1}) is usually much higher than σ_m (≈ 0.5 m s^{-1}), the total observation error is not minimized. On the other hand, reducing the energy per pulse to obtain a higher number of shots to reduce the σ_s contribution to σ_o is limited by the resulting decrease in the percent of good returns (P) and the increase in σ_m. Figure 3 illustrates the sense of the trades based on the above considerations. The optimum solution will vary significantly with mission requirements. For example, a PBL/cloud mission (high SNR potential) might require lower energy per pulse and a higher prf, while for a mid- and upper-tropospheric mission (marginal SNR potential), a higher pulse energy would probably be desirable.

f. Simulated performance profiles

In an attempt to express the anticipated performance of the LAWS instrument, a LAWS simulation model (see section 3) has been used to generate

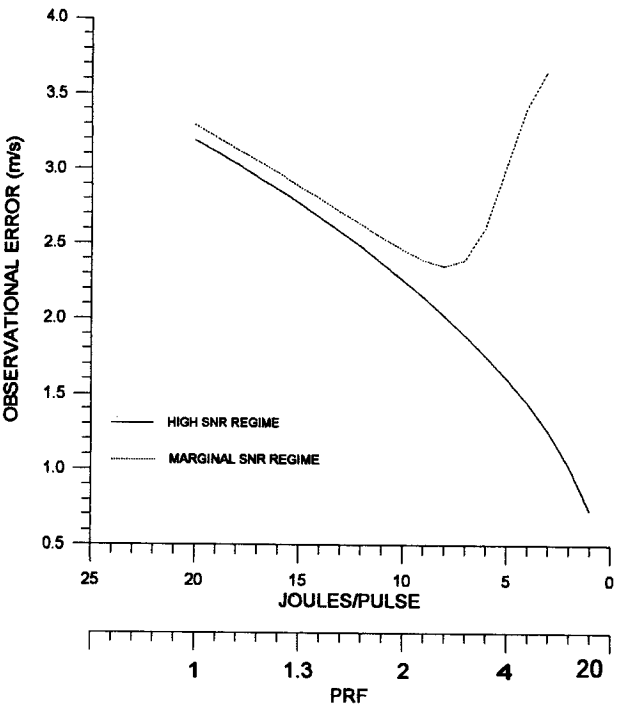

FIG. 3. The observational error within a 100 × 100 × 1 km^3 volume is shown as a function of the energy/pulse (in J) and the pulse repetition frequency (in Hz) for fixed power from the spacecraft. In this example, the instrument error σ_m was taken to be 1 m s^{-1} and the total rms variation in the wind field on all scales below 200 km was set at $\sigma_s = 3$ m s^{-1}. The high SNR regime was the continental PBL and the marginal SNR regime was the aerosol at 700 mb.

profiles of successful observations including the effects of dense clouds, semitransparent cirrus, and overall lidar sensitivity to aerosols. A backscatter distribution (Fig. 4) has been generated using analysis fields from the European Centre for Medium-Range Weather Forecasts (ECMWF), cloud statistics from *Nimbus-7,* and International Satellite Cloud Climatology Program observations, and aerosol data provided by the GLOBE and Air Force Geophysics Laboratory (AFGL) atmospheric transmission model (LOWTRAN 7) (Kneizys et al. 1988). The global variations in aerosol backscatter and molecular attenuations are driven by the relative humidity, temperature, pressure, and surface winds at each grid point in the ECMWF model fields. The distribution of attenuated backscatter at 9.11 μm shown in Fig. 4 (horizontal and vertical) is for a 24-h simulation. Note that this distribution includes backscatter from clouds using a relationship between cloud-top temperature and scattering (Del Guasta et al. 1993).

The performance profile in Fig. 5a resulted from simulating the returns from approximately 4 × 10^5 shots taken during a 24-h period. Statistics were compiled as each shot passed through the five

reference atmospheric layers (<70-, 70–300-, 300–500-, 500–850-, and 850-mb surface). If a shot intercepted an opaque cloud and its calculated signal was sufficient enough to produce an LOS measurement with a ±1 m s^{-1} accuracy, an observation was recorded, the shot terminated, and the obscuration counters for lower layers incremented. If a shot intercepted a transparent cloud (e.g., thin cirrus), a return from that level was recorded for a sufficient signal and an attenuated pulse was propagated to the next level. If no clouds existed within the layer, an aerosol return was computed and, if ±1 m s^{-1} accuracy was computed, the aerosol counter was incremented.

Figure 5a suggests that we should expect, within the PBL, an LOS wind measurement at least 50%–60% of the time for an instrument deployed at 525-km altitude with a 20 J laser and a 1.5-m telescope. Although the aerosol returns are stronger from the PBL, there are more returns from the overlying layer (850–500 mb) due to the additional contribution of low-level clouds that obscure the lower PBL 15%–20% of the time. Given that the mid- and upper-tropospheric aerosol backscatter coefficients used in the LAWS design are for desert dust-free, nonvolcanic conditions, the performance in Fig. 5a is considered to be a conservative estimate for the LAWS performance.

While the probability of getting an acceptable LOS observation (i.e., within ±1 m s^{-1} of the true LOS component) may be only 50% for individual shots, it is still possible that a useful estimate of the u and v components of the wind within a specified volume (e.g., 100 × 100 × 1 km^3) could be obtained as long as the joint probabilities yield at least one good forward

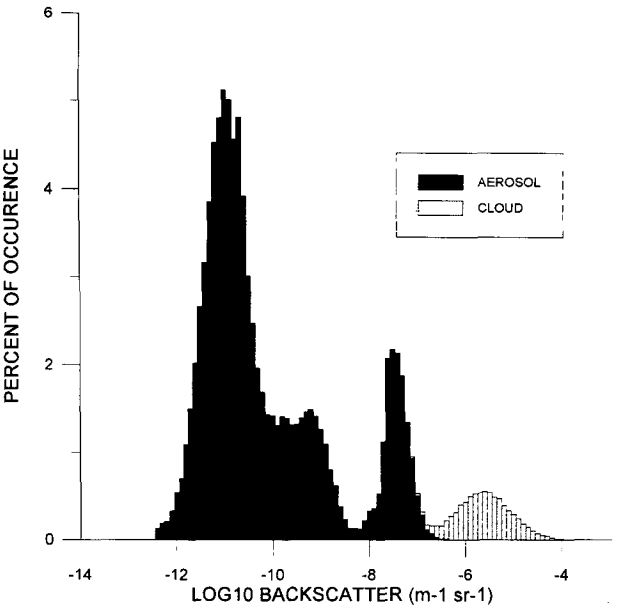

FIG. 4. The frequency distribution of LOS backscatter intensities at 9.11 μm for the entire globe during the month of January. The backscatter values above 2 km were based upon GLOBE data and below 2 km upon AFGL data (see section 2f). Clouds were those generated by the ECMWF model for a randomly selected 24-h period. A sample was defined by the average backscatter value for a 1-km layer within a 100 × 100 km^2 grid box not obscured by clouds.

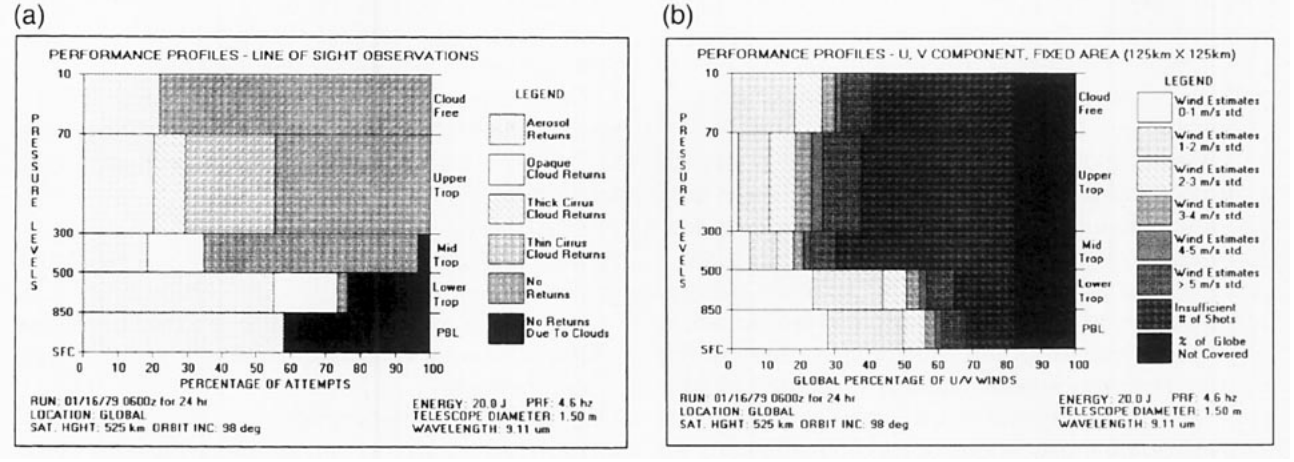

FIG. 5. (a) Vertical distribution of LOS observations that met the criteria of having a 98% probability of being within 1 m s^{-1} of the true LOS component of the wind computed from the ECMWF gridded wind fields. Criteria observations are labeled according to the backscattering media—aerosols, thick warm clouds, thick cold clouds, and thin cirrus. The percentages shown are based upon the number of shots taken and are not adjusted for global coverage by the instrument swath. (b) Vertical distribution of the horizontal wind component coverage and accuracies. The dark area to the right represents the percent of the globe not viewed by the lidar during a 24-h period. The vertical layers are chosen as the basis for general cloud types that would provide lidar returns and/or obscure lower-level data retrievals along the LOS. The interpretation of the figure should be as follows using the surface to 850-mb layer: ~29% of the 32,828 125 × 125 km^2 grid cells over the globe had velocity estimates that were within 1 m s^{-1} of the true average wind in each cell. In ~21% of those cells the velocity accuracy was between 1 and 2 m s^{-1}, etc.

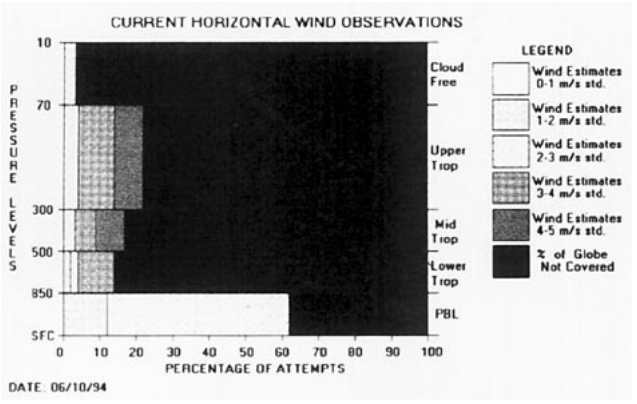

FIG. 6. Vertical distribution of the coverage and accuracy of direct wind measurements currently used in the NCEP operational global forecast model. Grid cells of 100 × 100 × 1 km^3 were used to compile the statistics. The accuracies are those assigned by the NCEP objective-analysis scheme. The "% of globe not covered" denotes that no observations were attempted during the 24-h period.

and one good aft shot. However, as discussed in section 2e, the accuracy (including representativeness) of target volume estimates depends upon the variability of the winds within the target area and the number of samples used to compute the u and v components. Figure 5b shows the distribution of u and v accuracies within the 100 × 100 × 1 km^3 volumes for the same time period as that used in Fig. 5a. The results are as one would expect: while most of the shots into the PBL may have high signal content, there are still too few shots to get 1 m s^{-1} component accuracy all of the time and, in the mid/upper troposphere, fewer shots with a good SNR lead to an increase in velocity measurement uncertainty.

g. Global coverage and accuracy of current wind observations

Currently, global models obtain directly measured wind data primarily from rawinsondes, surface land stations, ocean buoys, ship reports, aircraft reports, and satellite cloud tracking. Each observation system yields a data product of particular spatial coverage and accuracy. In general, the Northern Hemisphere is better observed over the landmasses than is the Southern Hemisphere and most of the oceans (Northern and Southern Hemisphere). Inspection of global maps showing the locations of wind observations for any 24-h period leads to the conclusion that there is a critical lack of direct wind observations over the oceans and most of the Southern Hemisphere. What little wind data are available are generally biased to cloudy regions and populated land areas.

To facilitate a comparison between current global coverage of wind observations and that expected from a Doppler wind lidar, the vertical distribution of current data collected within 111 km × 111 km areas from the National Centers for Environmental Prediction (formerly NMC) database during a 24-h period (e.g., 10 June 1994) has been constructed in Fig. 6. The accuracy (including representativeness) of each system's observations has been used to express the quality of the current measurements. The substantial amount of surface observations is from the Special Sensor Microwave/Imager, which provides ocean-surface wind speed data. The significant enhancement in the wind-observing capability with a wind lidar may be seen by comparing Fig. 6 with Fig. 5b.

h. Expected data products

Horizontal wind field estimates will be computed directly from lidar returns as well as derived from general circulation models after the assimilation of LOS observations and other data. To obtain the horizontal wind field directly from lidar data, acceptable LOS estimates from within a specified region will be combined to produce the two-dimensional wind field estimate. The size of the region will vary with the density of good shots; when backscatter values are high (e.g., $\beta \geq 7 \times 10^{-11}$ m^{-1} sr^{-1}), it is anticipated that horizontal wind estimates would be obtainable for 100-km grid boxes. In cleaner regions (e.g., $\beta < 7 \times 10^{-11}$ m^{-1} sr^{-1}) the grid-box size may have to be expanded to 300 km or so to obtain acceptable estimates of the horizontal wind.

The lidar data products, such as those from the LAWS instrument, would be unlike any wind measurement currently used. Several levels of data processing are anticipated to meet the needs of a diverse set of users. Table 2 summarizes six types of data that have been defined.

There are several attributes of lidar observations and characteristics that will require modification to data assimilation systems that have been designed for scalar quantities:

1) LOS wind components individually provide incomplete information on the total wind vector (i.e., more than one perspective is required to resolve the horizontal wind components from LOS wind components).
2) Each LOS wind observation will be accompanied by a quality flag such as one based upon the signal strength and the signal-processing algorithm used.
3) Within each range gate, the aerosol structure (gradient) will cause errors in the height assignment of the wind estimate (Emmitt and Wood 1989). However, these height-assignment errors will be significantly less than those associated with current passive techniques for cloud-motion winds.

1) LOS WIND COMPONENTS—NONGRIDDED

While the plan for processing lidar data is to retain the raw data (level 0) for reprocessing, most users will probably be interested in data products processed at levels 1–4. The level 1 product will be the LOS wind component (m s^{-1}) for individual range gates (or aggregated range gates) along with the related lidar shot geometry, signal strength, and other housekeeping information. In the mid- and upper troposphere it is likely that signals over more than the target depth of 1 km will have to be combined to produce acceptable wind estimates. Within the PBL, it may be possible, under undisturbed conditions, to achieve a higher vertical resolution of 300–500 m.

2) HORIZONTAL WIND COMPONENTS—NONGRIDDED (LEVEL 2)

Each LOS, by itself, is not a particularly useful observation. Only when several LOS observations from two or more geometrical perspectives are available can a unique estimate of the horizontal wind components be made. This also assumes that the average vertical motion within each shot volume is approximately zero.

While many users may want the wind products derived from a general circulation model that has assimilated the LOS observations (Lorenc et al. 1992) along with all other observational data (level 4), there will be others who want *u* and *v* wind components derived directly from a set of LOS observations (level 2). Algorithms have already been developed (Houston and Emmitt 1986) to produce a nongridded dataset of *u* and *v* components based upon optimal pairing of forward and aft shots. This would be the highest resolution data product available and could be as high as approximately 50 km in regions of abundant backscatter.

3) HORIZONTAL WIND COMPONENTS—GRIDDED (LEVEL 3)

Usually, more than just two LOS observations will need to be combined to estimate the wind for a grid cell. Generally, the minimum number of shots that are needed to make an accurate gridded wind field is six—three from one perspective and three from another. As a result, the level 2 product will be useful only where the SNR is high. Algorithms for producing the level 3 product have already been developed and are currently being used to generate input winds for the OSSEs described in section 3 (Wood et al. 1993).

4) MODEL-ASSIMILATED WIND PRODUCT—GRIDDED (LEVEL 4)

It is anticipated that for climate studies and weather forecasting, the LOS components, along with their individual quality flags, will be assimilated directly. In this process, the lidar winds will be blended with all other geophysical data and, therefore, contribute to the models' overall performance. Although the identity

TABLE 2. The data products expected from a full-capability wind lidar mission and their corresponding resolution and accuracy.

Product	Expected resolution	Expected accuracy
Horizontal vector winds	100 km—Horiz. 1 km—Vert. [300 m in high aerosol regions (e.g., PBL) or cirrus]	±1 to 5 m s^{-1} depending on aerosol amount with quality flags
Line of sight winds	6 per 100² km²—Horiz. 1 km—Vert. [300 m in high aerosol regions (e.g., PBL) or cirrus]	±1 to 5 m s^{-1} depending on aerosol amount with quality flags
Aerosol[1] distribution	100 km—Horiz. 1 km—Vert. [300 m in high aerosol regions (e.g., PBL)] Temporally averaged (e.g., daily)	TBD
Cirrus[2] distribution	100 km—Horiz. 300 m—Vert. Temporally averaged (e.g., daily)	TBD
Cirrus cloud-top height	50 km—Horiz.	±20–50 m[3]
Stratiform cloud-top height	50 km—Horiz.	±20–50 m

[1]Wavelength dependent.
[2]Cirrus not detectable by passive techniques (i.e., subvisible).
[3]Height determination for thin cirrus will be significantly more accurate than with current passive techniques.

of the observations is lost in this process, the gridded wind fields will be archived and distributed.

5) Cloud-top heights and backscatter coefficients

A Doppler lidar will be able to detect the presence of clouds and to measure cloud-top heights on a pulse-to-pulse basis. When the laser pulse encounters a cloud, the backscattered signal will be several orders of magnitude higher than the background atmospheric aerosol return. The high SNR will enable unambiguous detection of cloud presence, and should also facilitate measurement of cloud-top heights to expected accuracies of about 50 m. When the clouds are optically thin, as is usually the case for high ice clouds such as cirrus, the laser pulse will often be expected to completely penetrate the cloud. In such cases, a Doppler lidar will be able to identify multiple cloud layers and may be able to measure cloud-base heights, cloud thickness, and cloud backscatter coefficients.

Multiple scattering effects on the backscatter signals from clouds are not expected to be significant for Doppler lidars using coherent detection. The narrow, diffraction-limited transmitter divergence and receiver field of view (FOV) of the coherent lidar is a major factor in reducing effects of multiple scattering. The conclusion of Menzies et al. (1994) was that multiple scattering effects from clouds were negligible for a 9.25-μm airborne CO_2 coherent lidar for which the transmitter divergence and receiver FOV is larger than that of a typical space-based Doppler lidar design. Although the scattering efficiencies in most cloud types rise at the shorter wavelengths, multiple scattering is not expected to affect cloud height or Doppler measurements for a 2-μm coherent lidar either. The diffraction-limited transmitter divergence and receiver FOV are much smaller, scaling as the wavelength. Multiple scattering effects from clouds were obvious in some of the Lidar In-Space Technology Experiment (LITE) shuttle lidar data taken at 532-nm wavelength during nighttime conditions in its high sensitivity mode (i.e., when its FOV was 3.5 mrad). These effects were reduced, however, when LITE operated with its daytime FOV of 1.1 mrad (McCormick 1994, personal communication). A further reduction to a 0.03 mrad or smaller FOV of a space-based coherent Doppler lidar operating at 2-μm wavelength is certainly expected to reduce multiple scattering effects (for cloud penetration to maximum optical thicknesses of 3 or 4) to levels that are not problematic in signal interpretation.

Measurements of cloud and aerosol backscatter coefficients require an estimate of the backscattered signal intensity. For coherent lidar returns, obtaining a representative measurement of signal intensity is more difficult than measurement of frequency, even at high SNR, because of speckle (interference effects) in the backscattered signal. Lidar signal processing will have to include methods for smoothing and filtering the fluctuating signal intensity to extract cloud and aerosol backscatter coefficients and cloud-base-height estimates. Consequently, although cloud detection and cloud-top heights will be available for every laser pulse, the backscatter coefficient and cloud-base-height estimates (when obtainable) will generally be computed with a spatial resolution roughly equivalent to that of the velocity estimates. As mentioned in section 2h, when the aerosol backscatter coefficient is low ($\beta < 7 \times 10^{-11}$ m^{-1} sr^{-1}), more extensive spatial averaging will be required.

3. Observing system simulation experiments with lidar winds

Airborne lidars (Targ et al. 1991; Bilbro et al. 1986; Werner et al. 1989) have been in existence since the 1960s, but they have been primarily limited to examining technical issues or sub-synoptic-scale atmospheric phenomena. Thus, simulation studies have been necessary in order to meet the following objectives for a space-based wind lidar:

1) to develop the optimal lidar system design concept within specified constraints such as laser lifetime, platform power, and orbital parameters;
2) to develop algorithms for managing the use of the lidar shots and processing the lidar returns;
3) to evaluate various lidar system configurations and platform orbits in terms of their potential impact on global climate studies or weather forecasting; and
4) to provide simulated datasets for use in developing GCM data assimilation schemes.

LAWS Observing System Simulation Experiments (OSSEs) have been used to assess lidar system design trades or to conduct analysis/forecast impact tests with simulated LAWS observations. A LAWS simulation model was developed by NASA for use with the OSSEs. The major components are shown in Fig. 7 and described in detail in Wood et al. (1993).

a. OSSE results

Most remote-sensing instrument programs must address the twin issues of "what are the mission science objectives?" and "what are the minimum instrument design requirements to meet those objectives?" In the case of LAWS, the objectives were not expressed in quantitative terms such as "to improve

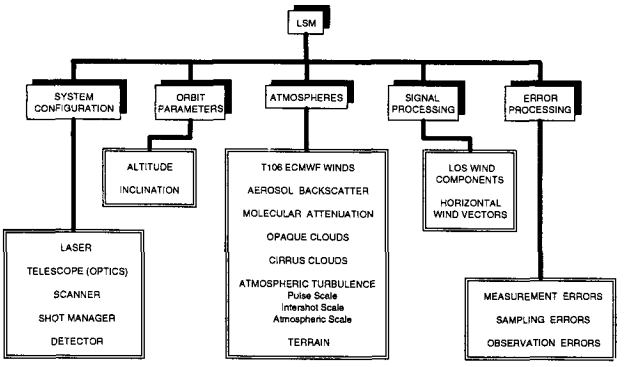

FIG. 7. A component diagram of the LAWS simulation model (LSM) used in OSSEs and other system design studies.

the 5-day forecast skill by 20%" or "to reduce the moisture transport error by 50%." Instead, the process of defining the mission design requirements for the LAWS instrument was to answer the question, "What are the science returns for a mission with a lidar system that is within certain cost and risk limits?" To answer this question an extensive set of observing system simulation experiments, referred to as OSSEs, has been performed.

While details of OSSEs and related experiments can be found in Atlas et al. (1985), Arnold and Dey (1986), Dey et al. (1985), Isaacs et al. (1992), Grassoti et al. (1991), Hoffman et al. (1990), and Gauthier et al. (1993), here we wish to describe the general approach (Fig. 8) and highlight a few of the results.

Since 1985, more than 15 OSSEs in support of the LAWS instrument were conducted by NASA/Goddard Space Flight Center (GSFC) (Atlas et al. 1985; Atlas 1990), by NASA/GSFC and Simpson Weather Associates (SWA) (Atlas and Emmitt 1991), and by The Florida State University (FSU) using input datasets from NASA/GSFC and SWA (Rohaly and Krishnamurti 1993). Primary issues resolved by these experiments have been

- the relative benefits of a LAWS instrument in various orbits [e.g., 705-km vs 525-km sun-synchronous, 450 km at a 55° orbital inclination vs 200 km equatorial (space shuttle), etc.], and
- the relative benefits of LAWS with different pulse energies, shot density, and scan routines (e.g., conical, fixed quadbeam, and fixed bibeam).

In general, the OSSEs led the former LAWS Science Team to converge on a polar sun-synchronous deployment at 500–550-km altitude. The OSSEs clearly showed that the current dearth of wind observations over the oceans, and, in particular, the Southern Hemisphere would allow even a modest lidar to have a very significant scientific impact as highlighted in section 4.

1) GODDARD SPACE FLIGHT CENTER OSSEs

OSSEs related to Doppler lidar measurements have been conducted at NASA/GSFC since 1983. The initial experiments were aimed at assessing the potential impact of an idealized Doppler wind lidar on numerical weather prediction. For this purpose, five assimilation experiments were run: 1) a control cycle, in which only conventional data were assimilated; 2) a First GARP (Global Atmospheric Research Program) Global Experiment (FGGE) cycle, in which conventional and special FGGE datasets, including Television Infrared Observational Satellite-N (TIROS-N) temperature soundings and geostationary satellite cloud-track winds, were assimilated; 3) a control plus TIROS temperature profiles experiment; 4) a control plus cloud-track winds experiment; 5) and an experiment that used data from the control plus satellite lidar wind profiles.

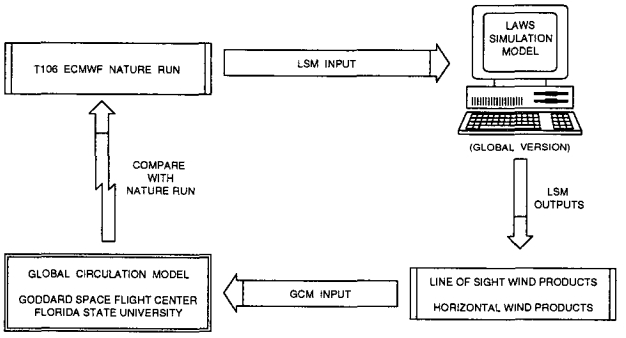

FIG. 8. Flow diagram for observing system simulation experiments designed to study the relative impact of various LAWS system configurations, scan patterns, shot management schemes, and orbits.

Figure 9 (from Atlas et al. 1985) summarizes the results for these initial simulation experiments. Here, S1 skill scores, averaged for eight forecast cases, are presented for the Southern Hemisphere. *These results indicated a significant improvement in forecast accuracy resulting from the assimilation of simulated satellite wind data and showed that wind data are more effective than temperature data in controlling analysis error.* In the Northern Hemisphere, the influence of simulated wind profiles was smaller but on occasion showed a significant positive impact.

More recent OSSEs have been conducted to evaluate the critical issues related to the design of a Doppler lidar system and its data utilization. One set of experiments, presented at the Global Energy and Water

Cycle Experiment Workshop on Temperature and Humidity Profiles from Space (Atlas 1990), evaluated the impact of lidar winds relative to very accurate temperature and moisture profiles. *These experiments demonstrated the importance of all three types of data, but showed the potential impact of lidar winds on atmospheric analysis and prediction to be substantially larger than either of the other types of observations.*

A second set of experiments was performed to determine the impact on data assimilation of changing the orbit for a lidar deployment from polar to 55° inclination, and the impact of lowering the altitude from 705 to 450 km. Changing the orbit inclination (e.g., to 55°) was suggested in order to benefit studies of diurnal processes and tropical and midlatitude circulation. Deploying a wind lidar at a lower altitude (e.g., 450 km) would increase the SNR of the returns.

The results from these experiments, which were presented at the American Meteorological Society's Second Symposium on Global Change Studies (Atlas and Emmitt 1991), showed that changing the orbit inclination would result in a substantial degradation near the South Pole. The impact of orbit altitude was found to be negligibly small.

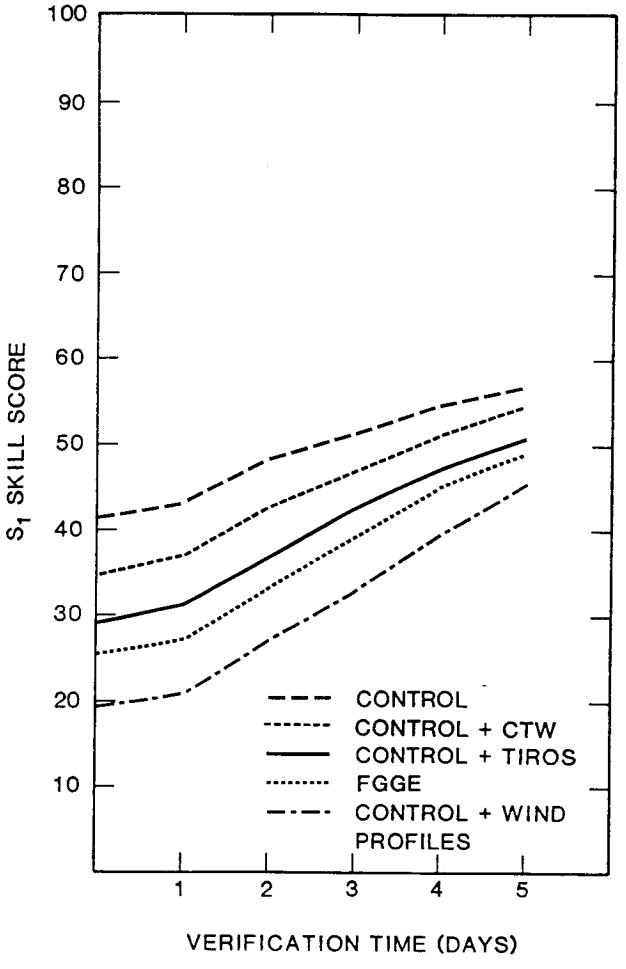

FIG. 9. Improvement in accuracy relative to the control of different types of simulated satellite data on Southern Hemisphere 500-mb height forecasts. (Lower S1 score indicates higher accuracy.)

2) OSSEs AT THE FLORIDA STATE UNIVERSITY

The FSU global modeling group also assessed the potential analysis/forecast impact of the LAWS instrument. A four-dimensional data assimilation system was used to update the initial conditions for a global general circulation model. The optimum interpolation objective analysis scheme used was very similar to the gridpoint analysis scheme formerly used at the National Centers for Environmental Prediction (Dey and Morone 1985). The FSU global spectral model was used at two different horizontal spectral resolutions, triangular truncation T42 (~314 km) and T106 (~125 km) (Krishnamurti et al. 1989).

The OSSE results of the FSU group were similar to those of NASA/GSFC. A significant improvement was found in both the analyses and forecasts for the Southern Hemisphere and the tropical oceans (e.g., Krishnamurti et al. 1991; Rohaly and Krishnamurti 1993). In the upper troposphere, the analysis error in the wind field was reduced by roughly 2 m s^{-1} globally when simulated LAWS observations were added. The midtropospheric height analysis was also improved.

In the lower troposphere, the wind analysis error was decreased by 1 m s^{-1} globally. The FSU OSSEs, in agreement with those of NASA/GSFC, have clearly shown that wind measurements will greatly benefit the understanding and prediction of the polar regions, the Southern Hemisphere, and the tropical oceans.

b. Other simulation studies

Tropical cyclone intensity has been shown to be quite sensitive to the flux convergence of angular momentum into a cyclone (Molinari and Vollaro 1990; DeMaria et al. 1993). This quantity can be calculated knowing the wind field alone. A "diagnostic OSSE" was carried out to test the ability of lidar winds to reproduce angular momentum flux convergence during the life cycle of Hurricane Elena (1985). Lidar winds at 200-km resolution were simulated from actual analyses at a single analysis level. Both random and nonrandom errors were added, the latter due to the 90-min time differences between adjacent swaths. These simulated LAWS winds, unaccompanied by any supplemental data sources, were objectively analyzed. Angular momentum flux convergence was calculated for 12 observation times for Hurricane Elena, and the results compared to a control analysis. Figure 10 shows a time series of the results. The

simulated lidar winds did remarkably well in reproducing control values throughout the life cycle of the storm.

4. Anticipated advances in earth system science with lidar winds

A Doppler wind lidar is the only space-based instrument that can provide direct measurement of the global tropospheric wind field. Such winds would significantly increase the skill of numerical weather forecasts and provide data that are fundamental to advancing the understanding and prediction of possible climate change as discussed below.

a. Doppler lidar winds and the U.S. Global Change Research Program and Intergovernmental Panel on Climate Change objectives

The Committee on Earth and Environmental Sciences (1989) outlined a framework for the U.S. Global Change Research Program (USGCRP). Leading the priority in research topics were Climate and Hydrologic Systems and Biogeochemical Dynamics, both of which require improved determination of atmospheric fluxes and the wind field. The USGCRP also contributes climate change studies within the framework of the Intergovernmental Panel on Climate Change (IPCC). The first IPCC report assessed prospects for investigating climate change (IPCC 1990). The IPCC recommended that five of the most critical areas for intensive study are 1) control of the greenhouse gases by the earth system; 2) control of radiation by clouds; 3) precipitation and evaporation; 4) ocean transport and storage of heat; and 5) ecosystem processes. There is a clear mandate to refine our understanding of the hydrologic and biogeochemical cycles. We need to better quantify the transports, phase changes, and chemical processes that interconnect the component subsystems of the planet. Wind data are fundamental to all of these calculations. The Doppler wind lidar stands as the unique sensor system capable of providing the required global measurements of this key parameter.

1) The hydrologic cycle

On climate timescales (e.g., a month or longer), the atmospheric branch of the earth's hydrologic cycle can be expressed as a balance between the column-integrated convergence of water vapor and net evaporation minus precipitation. The spatial and temporal variability in the components of this balance has great importance and, unfortunately, substantial uncertainty (Chahine 1992). Coupled with water vapor measurements from passive microwave and infrared sounders, Doppler lidar wind data could play a unique role in isolating this fundamental component of the earth's energy cycle. Furthermore, Doppler lidar wind measurements and other estimates of evaporation minus precipitation are strongly complementary. Calculation of flux convergence of water vapor using winds would serve as an independent check on estimates of evaporation minus precipitation; given any two measurements the third can be found as a residual. For

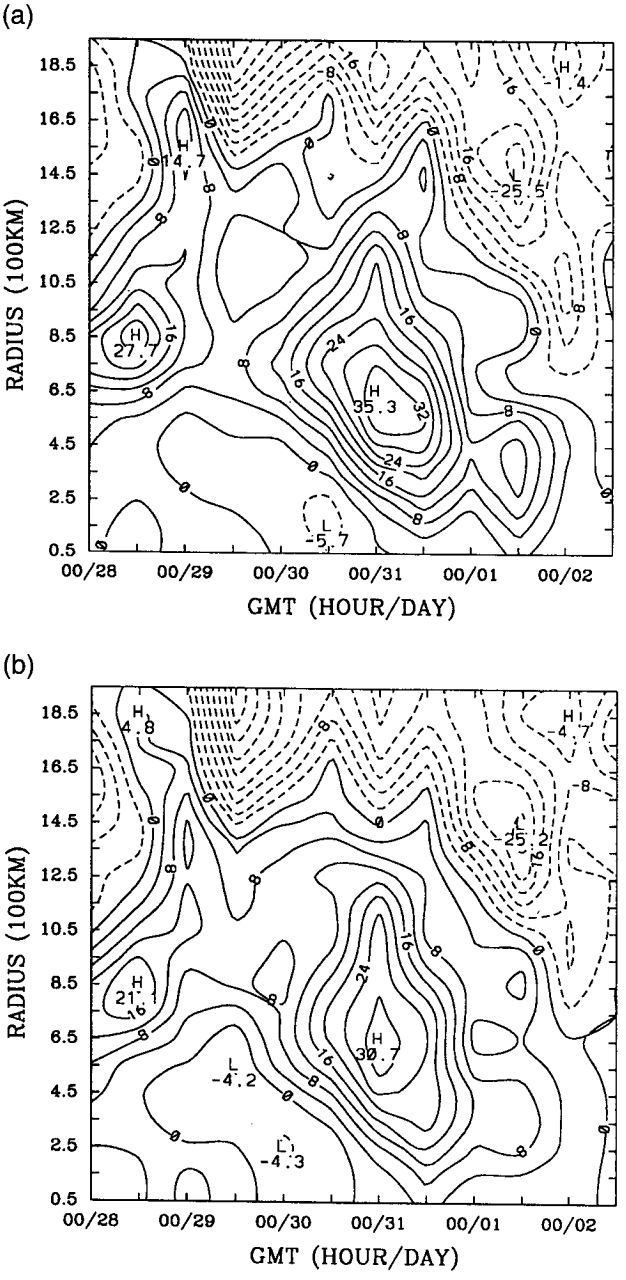

Fig. 10. Radius–time plot of the azimuthal eddy flux convergence of angular momentum for Hurricane Elena (1985). Contour interval 4 m s^{-1} day^{-1}. (a) From the control analysis; (b) from analysis of simulated lidar winds.

example, using moisture convergence estimated from Doppler lidar winds and water vapor estimates from the Multifrequency Imaging Microwave Radiometer (MIMR)/Microwave Humidity Sounder/Atmospheric Infrared Sounder and precipitation measurements from the Tropical Rainfall Measuring Mission, the resulting required evaporation could be obtained. Conversely, moisture convergence plus evaporation estimates from MIMR and SeaWinds, an EOS scatterometer, would yield the required precipitation amounts. This would be a powerful approach toward reducing the uncertainty in this fundamental cycle.

As stressed in both the USGCRP and IPCC documents, a major uncertainty in modeling climate scenarios, past, present, and future, is uncertainty in representing clouds. On all scales, cloud-system dynamics are strongly linked to the circulation patterns. Thus, to verify performance and integrity of climate models, it is necessary to improve the understanding of not only cloud and water vapor distributions, but vertical and horizontal transport of water vapor.

In addition to wind measurements, a Doppler lidar would also contribute key information on cloud-top height and, in many cases, cloud thickness. This vertical structure information, especially for ice clouds, is complementary to passive sounder and imager data and would contribute to a more accurate determination of cloud influence on radiative flux profiles.

2) Closure on atmospheric–oceanic heat transport

Top-of-the-atmosphere radiative fluxes provide a quantitative estimate of heat energy transport plus storage by the earth system. Partitioning of heat transport by oceanic and atmospheric components remains an unresolved question of major significance in climate dynamics. Despite the intensive measurement campaign planned for the World Ocean Circulation Experiment in the late 1990s (World Climate Research Program 1986), observational constraints will likely remain a barrier to sufficiently accurate measurement of global oceanic heat storage and transport for the foreseeable future. By appealing to Doppler lidar wind measurements and to profiles of temperature and moisture from passive sounders, the total energy transport requirement, determined from top-of-the-atmosphere net radiative fluxes, can be resolved into an atmospheric component and, by residual, an oceanic part. Current top-of-the-atmosphere flux uncertainties are of the order 10 Wm^{-2}, while those of the calculated atmospheric–oceanic transport are typically a factor of 3 to 5 larger over much of the globe. A large part of this uncertainty is due to errors in the wind analyses (Fortelius and Holopainen 1990).

3) Aerosols and the carbon cycle

One of the more striking shortfalls in global climate modeling continues to be the treatment of aerosols. Although their increase in generally thought to enhance cooling due to increased albedo (order 1 Wm^{-2}), an adequate understanding of their production, transport, radiative impact, and deposition is only rudimentary at best. Production by anthropogenic (industrial sources, fossil fuel burning) and natural processes (volcanic and biogenic emissions and aeolian transport) is widely distributed. Many important radiatively active aerosols have atmospheric residence times on an order of one week (Penner et al. 1992), and thus their dispersion depends critically on the evolving wind field. The atmospheric transport, interaction with clouds and radiation, and removal by precipitation requires better knowledge of the wind field (trajectory modeling) coupled with hydrologic modeling (scavenging by precipitation processes). Contemporary research into processes governing the carbon cycle has focused on searching for a "missing sink" of approximately 1.0–2.0 G of carbon per year (IPCC 1990). Methodologies to investigate the carbon budget have used inversion methods (Enting and Mansbridge 1989) as well as direct transport models (Tans et al. 1990). Both approaches rely upon the a priori specification of the wind field, the former in solving for sources/sinks required to explain the observed CO_2 concentrations and the latter in direct calculation of CO_2 distributions resulting from measured or modeled sources and sinks. Because the wind field is poorly measured over critical source/sink regions, such as tropical rain forests and boreal ecosystems, refinement in transport estimates via lidar wind measurements would be an important contribution to narrowing the uncertainties in the carbon cycle.

b. Impact of deforestation on rainfall

To highlight the significance of the present uncertainties in the tropospheric wind analyses for conducting climate change research, consider the findings summarized in Table 3 concerning the impact of deforestation on rainfall. The present uncertainties in the tropospheric wind field alone produce corresponding uncertainties in the moisture budget that match or exceed the drying effect found in deforestation experiments with GCMs. *Without the measurements of the ageostrophic wind (the wind component crucial for accurate transport calculations), our present level of uncertainty in the water vapor flux divergence calculations will not improve substantially.*

c. Planetary-scale dynamics and climate

The coupling of the moisture cycle with radiative processes and surface heterogeneity leads to an

TABLE 3. Sensitivity of the moisture flux divergence to uncertainties in tropospheric wind analyses, contrasted with the effect of Amazonian deforestation (rain forest replaced with grassland)* on rainfall (based on findings of Wang et al. 1992).

Region	Current wind analysis uncertainties	Resulting uncertainties in moisture flux divergence (for precipitable water)
North America	2.3 m s^{-1}	2.1 cm $month^{-1}$
South America	3.0 m s^{-1}	4.9 cm $month^{-1}$
Effect on Amazonian rainfall		≈4.0 cm $month^{-1}$ (~20%–25% reduction)

*See Lean and Warrilow 1989; Shukla et al. 1990.

exceedingly complex thermodynamic forcing of the climate. As gradients of temperature are generated by differential heating, a continual process of equilibration is necessary. The global wind field plays a dominant role in this response. To understand the essential modes of dynamical behavior that characterize climate, it is not sufficient to know the mean thermodynamic state or even a succession of states. It is necessary that the horizontal and vertical fluxes of heat, moisture, momentum, etc. be accurately measured. Air-surface fluxes are parameterized with respect to surface winds. The winds in the planetary boundary layer are difficult to calculate in a GCM. This leads to a systematic error of about 10%–20% in the winds and fluxes (Foster and Brown 1994). Observations are needed to get these winds correct and satellite lidar winds are needed to obtain sufficient data for global flux analyses. The shortcomings of the current observing system are well documented (Brown and Foster 1994; Randall et al. 1992). Furthermore, both the rotational and divergent components of the flow must be accurately determined, and only the direct measurement of the wind from satellites can provide the divergent component with sufficient accuracy.

d. Aerosols, trace gases, and the biogeochemical cycle

Next to water in importance to life on earth are compounds involving carbon, nitrogen, and sulfur. There is abundant evidence that increases are occurring in the atmospheric composition of radiatively active trace gases composed of these elements, including carbon dioxide, methane, oxides of nitrogen and sulfur, as well as the chlorofluorocarbons (IPCC 1990). Many of these changes are thought to be a result of human activities superimposed on natural fluctuations, but the complex causes and relationships are not yet fully understood. Whatever the cause of these increases, the resulting changes in regional and global climates over the next 100 years could possibly exceed those experienced by mankind. Thus, there is an urgent need to understand the biogeochemical cycles of these elements. The same processes that are needed to better define the hydrologic cycle will also be critical in estimating the long-range transport of trace gases and aerosols. An example for which global wind data would be valuable is in understanding the possible role of tropospheric dynamics in modulating the ozone hole during the Southern Hemisphere stratospheric spring. Global wind data should also be of value in studies of the influence of transient waves on the stability of the northern polar vortex.

e. Critical role of wind measurements for NWP

As mentioned above, accurate, global wind measurements would be as valuable for weather forecasting as they would be for climate studies. The relatively advanced state of atmospheric general circulation models now available for coupling with those of the ocean and biosphere is due in large part to the advances in numerical weather prediction (NWP), for which atmospheric general circulation models are now widely used. In addition, improvement in NWP is essential for improving the validation of climate models. Our understanding of the evolution of the atmospheric component of climate is ultimately based on the continuous assimilation of data into NWP systems. A number of observing system simulation experiments, where simulated Doppler lidar winds have been used in general circulation models, have consistently indicated that a dramatic improvement in weather forecasting skill would occur with the addition of lidar winds in data-sparse regions (see section 3a). In addition to the obvious fact that accurate observations in data-sparse regions will always be useful, one can mention at least two independent reasons for such an improvement.

First, even if mass observations are already available, which can lead to wind estimates through the geostrophic relationship, those estimates cannot be expected to be as accurate as estimates obtained from the direct measurement of the wind. This is especially true because differentiation worsens the effect of noisy observations. Since the geostrophic relationship relates the wind to the horizontal pressure gradient, this is a major cause of error in the estimation of the wind field (Kalnay et al. 1985).

A second reason is that at low latitudes and at small scales at higher latitudes, the geostrophic relationship is often invalid so that winds become an increasingly more important measure of the atmospheric state. The next generation NWP models (in the time frame of the first space-based Doppler wind lidar) will reach high-enough resolution to include significantly nongeostrophic scales.

f. Dynamics of weather systems

The assimilation of Doppler lidar winds along with other available data would also provide four-dimensional, dynamically consistent datasets with sufficient resolution to allow a detailed diagnostic study of cyclones and anticyclones, fronts, jets, shear lines, and convergence zones throughout their life cycle. Furthermore, by means of the data-assimilation process, lidar winds should improve the analysis of other variables, as well as model diagnostic quantities. Reviews of recent examples of the use of datasets derived from regional-scale models for the study of subsynoptic phenomena are described by Keyser and Uccellini (1987) and Anthes (1988), while an example of the use of a global model for the study of oceanic cyclogenesis is given in Atlas (1987). Many of these studies were limited by the lack of accurate wind data over the oceans. For example, in the Atlas (1987) study, upper-level cloud-track wind data were found to degrade the model simulation of cyclogenesis. Doppler lidar winds afford an unprecedented opportunity to advance knowledge of extratropical weather systems.

Some examples of longstanding research problems in the dynamics of extratropical weather systems in which the application of datasets incorporating lidar wind measurements should prove useful are 1) continuous documentation of the frontal structure throughout the cyclone life cycle; 2) the nature of interactions between upper- and lower-tropospheric processes in cyclogenesis and frontogenesis; 3) the origin of antecedent disturbances (e.g., jet streaks) that contribute to cyclogenesis; 4) the relationship of cyclones and fronts to the larger scales; and 5) the nature and dynamics of lateral interactions between flow regimes (e.g., through phasing and merger).

While cyclogenesis has been studied in detail in selected regions, the efforts have generally been limited to data-rich continental areas and adjacent coastal oceanic areas. The opportunity exists to extend descriptions of the structure and evolution of cyclones in maritime regions, especially in the Southern Hemisphere. Until comparatively recently, the extent to which cyclogenesis involved the interaction between upper- and lower-level disturbances or occurred in isolation of the influence of upper-level features was uncertain (Petterssen et al. 1962; Petterssen and Smebye 1971). Although the former scenario is now accepted to be the more common, the relative importance of upper- versus lower-level processes has not been documented in a global, climatological sense.

In particular, cyclone structure and evolution have not been examined in detail in three-dimensions (particularly in the vertical) over the oceans. Uncertainties resulting from the lack of upper-air data have resulted in a view that low-level cyclone structure is rich in mesoscale detail, whereas upper levels are synoptic scale (Reed and Albright 1986). This also can result in the fictitious representation of the lower-tropospheric thermal structure as represented in thickness patterns, since a finescale surface height analysis subtracted from a synoptic-scale 500-mb height analysis can introduce a warm-core structure. Lidar wind observations would contribute substantially to understanding this phenomenon.

In addition, the horizontal and vertical resolution of lidar winds would allow a better definition of the potential vorticity structure of the midlatitude troposphere and the structure of the tropopause than has previously been possible. This advance would allow detection of antecedent features (e.g., jet streaks) that may eventually interact with low-level features resulting in cyclogenesis.

Global datasets over long time periods would allow revisions to cyclone climatologies, especially in maritime regions and the development of a climatology of cyclones in relation to the large-scale flow. Parameters of interest are the geometry of the circulations (aspect ratio) and characteristic scales as a function of life cycle.

Finally, theoretical studies of cyclogenesis emphasize amplification of a small-amplitude perturbation based on linear stability analysis of a basic-state flow consisting of a zonal jet with meridional and vertical shear. These studies need to incorporate more general basis states (i.e., polar/subtropical) and finite-amplitude initial perturbations. Focused observational studies based on lidar winds have the potential of defining the basis and initial states for cyclogenesis to help guide future theoretical developments.

g. Economic benefits

In addition to the important scientific advances that would be achieved with the deployment of a Doppler wind lidar, as discussed above, there is a substantial evidence that a significant economic benefit to the nation would occur with the use of lidar wind data for operational weather forecasting. Two notable examples would be the reduction in fuel consumption by the airlines achieved through more accurate wind fore-

casts in the upper troposphere and in improving hurricane track and intensity forecasts and thereby reducing the area of overwarning for hurricane landfall.

First, it has been estimated that a 1% reduction in fuel consumption would result in a yearly savings of about $100 million (Steinberg 1983). Second, the National Hurricane Center has estimated (Sheets 1990) that preparation/evacuation costs incurred in the coastal areas covered in a hurricane warning are about $90,000 per kilometer. Typically, more than 350 km of coastline is "overwarned" because of uncertainties in the forecast track. In tests with a barotropic model, Franklin and DeMaria (1992) evaluated the impact of omega dropwindsondes (ODWs). They found that the mean forecast error was reduced by 12%–16% with data from the ODWs at 24–36 h prior to landfall, when the decision of whether to issue a hurricane warning is made.

5. Concluding remarks

The technology to deploy a space-based Doppler wind lidar is now available. The deployment of such an instrument would fundamentally advance the understanding and prediction of weather and climate. Also, a significant economic benefit may be expected with the use of lidar wind observations for operational weather forecasting.

Because of budgetary constraints, the deployment of the LAWS-type (e.g., ~20 J) instrument discussed in this paper does not appear likely in the near future. On the other hand, preliminary analyses indicate that significant science advances can be expected with a small-satellite version of LAWS. Furthermore, recent advances with the 2-μm solid-state lidar now make that technology competitive for a small-satellite mission. These topics are the primary focus of the NOAA Working Group on Space-Based Lidar Winds and personnel at the NASA/Marshall Space Flight Center.

Acknowledgments. The support of NASA Headquarters for the original LAWS program is sincerely acknowledged, especially the advice and encouragement of John Theon and Ramesh Kakar.

The efforts of personnel at the NASA/Marshall Space Flight Center, particularly those of Richard Beranek, Vernon Keller, Jeffery Rothermel, and Michael Kavaya, have been indispensable in helping assess the scientific impact of a variety of system trades (i.e., orbital altitude, inclination, etc.). The excellent work of the contractor teams on the instrument design studies was also critical, especially that of John Petheram and Dave Wilson, who headed the Martin Marietta Astro Space and Lockheed Missiles and Space Company teams, respectively.

Some of the information for this article was taken from the NASA EOS LAWS Instrument Panel Report, Volume II, Section II—Science Objectives. The report was one of the documents released as part of the NASA EOS Announcement of Opportunity in February 1988.

Dan Keyser made a number of useful contributions to section 4f of this paper. Sidney Wood and Linnea Wood were responsible for much of the software that was used to produce Figs. 4, 5, and 6. Eugenia Kalnay, Paul Long, Pierre Morel, Jim Yoe, and the anonymous reviewers also made several helpful suggestions that improved the manuscript.

In addition to some of the authors, the contributions to the LAWS Instrument Panel Report are sincerely acknowledged. Members of the panel included: Vincent Abreu, Richard Anthes, Wayman Baker, James Bilbro, David Bowdle, David Burridge, Robert Curran, George Emmitt, Sylvia Ferry, Dan Fitzjarrald, Pierre Flamant, Reynold Greenstone, R. Michael Hardesty, Kenneth Hardy, Milton Huffaker, Patrick McCormick, Robert T. Menzies, Richard Schotland, James Sparkman, Michael Vaughan, and Christian Werner.

Finally, the expert typing ability of Pam Brandts is sincerely acknowledged as well as her patience in correcting the numerous drafts. Angela Stansbury also provided expert assistance in preparing the manuscript.

References

Abreu, V. J., J. E. Barnes, and P. B. Hays, 1992: Observations of winds with an incoherent lidar detector. *Appl. Opt.*, **31,** 4509–4514.

Ancellet, G. M., R. T. Menzies, and D. M. Tratt, 1988: Atmospheric backscatter vertical profiles at 9.2 and 10.6 μm: A comparative study. *Appl. Opt.*, **27,** 4907–4912.

Anthes, R. A., 1988: Advances in the understanding and prediction of cyclone development with limited-area fine-mesh models. *Proc. Palmén Memorial Symposium on Extratropical Cyclones,* Helsinki, Finland, Amer. Meteor. Soc., 321–322.

Arnold, C. P., Jr., and C. H. Dey, 1986: Observing-systems simulation experiments: Past, present, and future. *Bull. Amer. Meteor. Soc.,* **67,** 687–695.

Atlas, R., 1987: The role of oceanic fluxes and initial data in the numerical prediction of an intense coastal cyclone. *Dyn. Atmos. Oceans,* **10,** 359–388.

——, 1990: Simulation studies of the impact of satellite temperature and humidity retrievals. Report of the First GEWEX Temperature/Humidity Retrieval Workshop, WMO/TD-460, 59 pp.

——, and G. D. Emmitt, 1991: Implications of several orbit inclinations for the impact of LAWS on global climate studies. Preprints, *Second Symp. on Global Change Studies,* New Orleans, LA, Amer. Meteor. Soc., 28–32.

——, E. Kalnay, W. E. Baker, J. Susskind, D. Reuter, and M. Halem, 1985: Observing system simulation experiments at GSFC. *Proc. NASA Symposium on Global Wind Measurements.* Columbia, MD, NASA, 65–71.

Banta, R. M., L. D. Olivier, and D. H. Levenson, 1993: Evolution of the Monterey Bay sea-breeze layer as observed by pulsed Doppler lidar. *J. Atmos. Sci.,* **50,** 3959–3982.

Bilbro, J. W., and W. W. Vaughan, 1978: Wind field measurement in the nonprecipitous regions surrounding severe storms by an airborne pulsed Doppler lidar system. *Bull. Amer. Meteor. Soc.,* **59,** 1095–1100.

——, G. Fichtl, D. Fitzjarrald, M. Krause, and R. Lee, 1984: Airborne Doppler lidar wind field measurements. *Bull. Amer. Meteor. Soc.,* **65,** 348–359.

——, C. A. Dimarzio, D. Fitzjarrald, S. Johnson, and W. D. Jones, 1986: Airborne Doppler lidar measurements. *Appl. Opt.,* **25,** 3952–3960.

Bowdle, D. A., 1986: A global-scale model of aerosol backscatter at CO_2 wavelengths for satellite-based lidar sensors. Preprints, *Second Conf. on Satellite Meteorology/Remote Sensing*

and Applications, Williamsburg, VA, Amer. Meteor. Soc., 303–306.

——, 1989: The global backscatter experiment. *Proc. Fifth Conf. on Coherent Laser Radar: Technology and Applications,* Munich, Germany, Deutsche Forschungsanstalt fur Luft-und Raumfahrt, 221–224.

——, J. Rothermel, J. M. Vaughan, D. W. Brown, and M. J. Post, 1991: Aerosol backscatter measurements at 10.6 micrometers with airborne and ground-based CO_2 Doppler lidars over the Colorado high plains: lidar intercomparison. *J. Geophys. Res.,* **96,** D3, 5327–5335.

——, D. R. Cutten, E. McCaul, and V. Srivastava, 1993: The Global Backscatter Experiment (GLOBE): Database analysis, and applications. Preprints, *Seventh Conf. on Coherent Laser Radar Applications and Technology.* Washington, DC, Opt. Soc. Amer., 131A–D.

Brown, R., and R. Foster, 1994: On large-scale PBL modeling. *Global Atmos.–Ocean System,* **2,** 163–183.

Capon, J., 1969: High resolution frequency-wavenumber spectrum analysis. *Proceedings IEEE,* **57,** 1408–1418.

Chahine, M. T., 1992: GEWEX: The global energy and water cycle experiment. *Eos Trans.,* **73,** 9.

Committee on Earth and Environmental Sciences, 1989: Our changing planet: The FY90 research plan, 118 pp.

Del Guasta, M., M. Morandi, and L. Stefanutti, 1993: One year of cloud lidar data from Dumont d'Urville (Antarctica) 1. General overview of geometrical and optical properties. *J. Geophys. Res.,* **98,** 18 575–18 587.

DeMaria, M., J.-J. Baik, and J. Kaplan, 1993: Upper-level eddy angular momentum fluxes and tropical cyclone intensity change. *J. Atmos. Sci.,* **50,** 1133–1147.

Dey, C. H., and L. L. Morone, 1985: Evaluation of the National Meteorological Center global data assimilation system: January 1982–December 1985. *Mon. Wea. Rev.,* **113,** 304–318.

——, W. J. Bostelman, and C. P. Arnold Jr., 1985: Design of a WINDSAT observing system simulation experiment. *Proc. NASA Symp. on Global Wind Measurements.* Columbia, MD, NASA, 73–79.

Emmitt, G. D., 1985a: Convergence and vorticity structures in convective storm outflows as detected by an airborne Doppler lidar velocimeter. *Proc. 14th Conf. on Severe Local Storms,* Indianapolis, IN, Amer. Meteor. Soc., 56–59.

——, 1985b: Convective storm downdraft outflows detected by NASA/MSFC's airborne 10.6 μm pulsed Doppler lidar system. Tech. Rep. on NASA/Marshall Space Flight Center, Contract NAS8-35597, 46 pp. [Available from NASA/Marshall Space Flight Center, Huntsville, AL 35812.]

——, 1987: Error analysis for total wind vector computations using one component measurements from a space-based Doppler lidar. *Proc. Fourth Conf. on Coherent Laser Radar: Technology and Applications.* Aspen, CO, Opt. Soc. Amer., 213–216.

——, 1993: Using ground-based coherent Doppler lidars to evaluate algorithms for shot management and signal processing of proposed space-based wind sounders. *Proc. Seventh Conf. on Coherent Laser Radar Applications and Technology,* Paris, France, Opt. Soc. Amer., 182–184.

——, and J. W. Bilbro, 1987: Assessment of error sources for one component wind measurements with a space-based Doppler lidar. *Proc. OSA Tropical Meeting on Coherent Laser Radar: Technology and Applications.* Aspen, CO, Opt. Soc. Amer., 217–219.

——, and S. A. Wood, 1989: Simulation of a space-based Doppler lidar wind sounder—sampling errors in the vicinity of wind and aerosol inhomogeneities. *Proc. Fifth Conf. on Coherent Laser Radar,* Munich, Germany, OSA/IEEE/SPIE/Amer. Meteor. Soc., 64–66.

——, and G. Séze, 1991: Clear line-of-sight (CLOS) statistics within cloudy regions and optimal sampling strategies for space-based lidars. *Proc. Seventh Symp. on Meteorological Observations and Instrumentation, Special Session on Laser Atmospheric Studies,* New Orleans, LA, Amer. Meteor. Soc., J100–J104.

——, and S. A. Wood, 1991: Simulated wind measurements with a low power/high PRF space-based Doppler lidar. *Proc. Optical Remote Sensing of the Atmosphere, Fifth Topical Meeting,* Williamsburg, VA, Amer. Meteor. Soc., 41–43.

Enting, I. E., and J. V. Mansbridge, 1989: Seasonal sources and sinks of atmospheric CO_2: Direct inversion of filtered data. *Tellus,* **41B,** 111–126.

Fortelius, C., and E. Holopainen, 1990: Comparison of energy source estimates derived from atmospheric circulation data with satellite measurements of net radiation. *J. Climate,* **3,** 646–660.

Foster, R., and R. Brown, 1994: PBL modeling for GCMs: A comparison between a two-layer similarity and higher order closure model. *Global Atmos.–Ocean System,* **2,** 199–219.

Franklin, J. L., and M. DeMaria, 1992: The impact of omega dropwindsonde observations on barotropic hurricane track forecasts. *Mon. Wea. Rev.,* **120,** 381–391.

Gauthier, P., P. Courtier, and P. Moll, 1993: Assimilation of simulated wind lidar data with a Kalman filter. *Mon. Wea. Rev.,* **121,** 1803–1820.

General Electric Astro Space, 1992: Definition and preliminary design of the Laser Atmospheric Wind Sounder. Final report on NASA/Marshall Space Flight Center study, Contract NAS8-36589, 273 pp. [Available from NASA/Marshall Space Flight Center, Huntsville, AL 35812.]

Grassoti, C., R. G. Isaacs, R. N. Hoffman, M. Mickelson, T. Nehrkorn, and J.-F. Louis, 1991: A simple Doppler wind lidar sensor: Simulated measurements and impacts in a global assimilation and forecast system. Phillips Laboratory Tech. Rep. 91-2253, 64 pp. [Available from Phillips Laboratory, Hanscom, MA 01731.]

Hall, F. F. Jr., R. E. Cupp, and S. W. Troxell, 1988: Cirrus cloud transmittance and backscatter in the infrared measured with a CO_2 lidar. *Appl. Opt.,* **27,** 2510–2516.

Hardesty, R. M., R. E. Cupp, M. J. Post, T. R. Lawrence, J. M. Intrieri, and P. J. Neiman, 1988: A ground-based, injection-locked, pulsed TEA laser for atmospheric wind measurements. *Proc. SPIE Symp. on Airborne and Spaceborne Lasers for Terrestrial Geophysical Sensing.* Bellingham, WA, SPIE, 23–28.

Henderson, S. W., P. J. M. Suni, C. P. Hale, S. M. Hannon, J. R. Magee, D. L. Bruns, and E. H. Yuen, 1993: Coherent laser radar at 2 μm using solid state lasers. *IEEE Trans. Geosci. and Remote Sens.,* **31,** 4–15.

Hoffman, R. N., C. Grassotti, R. G. Isaacs, J. Louis, T. Nehkorn, and D. C. Norquist, 1990: Assessment of the impact of simulated satellite lidar wind and retrieved 183 Ghz water vapor observations on a global data assimilation system. *Mon. Wea. Rev.,* **118,** 2513–2542.

Houston, S., and G. D. Emmitt, 1986: Assessment of measurement error due to sampling perspective in the space-based Doppler lidar wind profiler. Preprints, *Second Conf. on Satellite Meteorology/Remote Sensing and Applications.* Williamsburg, VA, Amer. Meteor. Soc., 523–525.

——, and ——, 1987: Impact of a space-based Doppler lidar wind profiler on our knowledge of hurricanes and tropical meteorology. Preprints, *17th Conf. on Hurricanes and Tropical Meteorology.* Miami, FL, Amer. Meteor. Soc., 182–185.

Huffaker, R. M., 1978: Feasibility study of satellite-borne lidar global wind monitoring system. NOAA Tech. Memo., ERL WPL-37, 276 pp. [Available from NOAA/Environmental Technology Laboratory, Boulder, CO 80303.]

——, R. T. Lawrence, R. J. Keeler, M. J. Post, J. T. Priestley, and J. A. Korrell, 1980: Feasibility study of satellite-borne lidar global

wind monitoring system, Part II. NOAA Tech. Memo., ERL WPL-63, 124 pp. [Available from NOAA/Environmental Technology Laboratory, Boulder, CO 80303.]

——, ——, M. J. Post, J. T. Priestley, F. F. Hall Jr., R. A. Richter, and R. J. Keeler, 1984: Feasibility studies for a global wind measuring satellite system (WINDSAT): Analysis of simulated performance. *Appl. Opt.*, **22,** 1655–1665.

Intrieri, J. M., A. J. Bedard, and R. M. Hardesty, 1990: Details of colliding thunderstorm outflows as observed by Doppler lidar. *J. Atmos. Sci.*, **47,** 1081–1098.

IPCC, 1990: Climate Change: The IPCC Scientific Assessment. WMO/UNEP Intergovernmental Panel on Climate Change.

Isaacs, R. G., C. Grassotti, R. N. Hoffman, M. Mickelson, T. Nehrkorn, J.-F. Louis, G. Molnar, and B. L. Linder, 1992: Assessment of spaceborne lidar for meteorological analyses. Phillips Laboratory Tech. Rep. 92-2205, 47 pp. [Available from Phillips Laboratory, Hanscom, MA 01731.]

Kalnay, E., J. C. Jusem, and J. Pfaendtner, 1985: The relative importance of mass and wind data in the present observing system. *Proc. NASA Symp. on Global Wind Measurements,* Columbia, MD, NASA, 1–5.

Kent, G. S., M. P. McCormick, and S. K. Schaffner, 1991: Global optical climatology of the free tropospheric aerosol from 1.0 μ satellite occultation measurements. *J. Geophys. Res.*, **96,** D3, 5249–5267.

——, G. K. Yue, U. O. Farrukh, and A. Deepak, 1983a: Modeling atmospheric aerosol backscatter at CO_2 laser wavelengths. 1: Aerosol properties, modeling techniques and associated problems. *Appl. Opt.*, **22,** 1655–1665.

——, ——, ——, and ——, 1983b: Modeling atmospheric aerosol backscatter at CO_2 laser wavelengths. 2: Modeled values in the atmosphere. *Appl. Opt.*, **22,** 1666–1670.

Keyser, D., and L. W. Uccellini, 1987: Regional models: Emerging research tools for synoptic meteorologists. *Bull. Amer. Meteor. Soc.*, **68,** 306–320.

Kneizys, F. X., E. P. Shettle, L. W. Abreau, G. P. Anderson, J. H. Chetwynd, W. O. Gallery, J. E. A. Selby, and S. A. Clough, 1988: User's guide for LOWTRAN 7. AFGL Rep. AFGL-TR-88-0177, ADA206773, 137 pp. [Available from Phillips Laboratory, Hanscom, Massachusetts 01731.]

Korb, C. L., B. M. Gentry, and C. Y. Weng, 1992: Edge technique theory and application to the lidar measurement of atmospheric wind. *Appl. Opt.*, **31,** 4202–4213.

Krishnamurti, T. N., D. Oosterhof, and N. Dignon, 1989: Hurricane prediction with a high-resolution global model. *Mon. Wea. Rev.*, **117,** 631–669.

——, J. Xue, G. Rohaly, D. Fitzjarrald, G. D. Emmitt, J. Houston, and S. Wood, 1991: Using a global spectral model in an observing system simulation experiment for LAWS—An EOS wind measuring system. Preprints, *Second Symp. on Global Change Studies,* New Orleans, LA, Amer. Meteor. Soc., 23–27.

Lean, J., and D. A. Warrilow, 1989: Simulation of the regional impact of Amazon deforestation. *Nature,* **342,** 411–413.

Lockheed, 1992: Design definition of the Laser Atmospheric Wind Sounder. Final report on NASA/Marshall Space Flight Center study, contract NAS8-37590. [Available from NASA/Marshall Space Flight Center, Huntsville, AL 35812.]

Lorenc, A. C., R. J. Graham, I. Dharssi, B. Macpherson, N. B. Igleby, and R. W. Lunnon, 1992: Preparation for the use of Doppler wind lidar information in meteorological assimilation systems. Final report on ESA study, contract 9063/90/HGE-I, 90 pp.

Marple, S. L., 1987: Minimum variance spectral estimation. *Digital Spectral Analysis with Applications,* Prentice-Hall, 350–357.

McCormick, M. P., H. M. Steele, P. Hammill, W. P. Chu, and T. J. Swissler, 1982: Polar stratospheric cloud sightings by SAM II. *J. Atmos. Sci.*, **39,** 1387–1397.

Menzies, R. T., 1986: Doppler lidar atmospheric wind sensors: A comparative performance evaluation for global measurement applications from earth orbit. *Appl. Opt.*, **25,** 2546–2553.

——, and R. M. Hardesty, 1989: Coherent Doppler lidar for measurements of wind fields. *Proc. IEEE,* **77,** 449–462.

——, and D. M. Tratt, 1993: Infrared lidar sensitivity to cloud optical and geometrical properties; Implications for Earth-orbiting Doppler lidar. *Proc. Seventh Conf. on Coherent Laser Radar Applications and Technology,* Paris, France, CNES, CNRS, ESA, 107–110.

——, G. M. Ancellet, D. M. Tratt, M. G. Wurtele, J. C. Wright, and W. Pi, 1989: Altitude and seasonal characteristics of aerosol backscatter at thermal infrared wavelengths using lidar observations from coastal California. *J. Geophys. Res.*, **94,** D7, 9897–9908.

——, D. M. Tratt, and P. H. Flamant, 1994: Airborne carbon dioxide coherent lidar measurements of cloud backscatter and opacity over the ocean surface. *J. Atmos. Oceanic Technol.*, **11,** 770–778.

Molinari, J., and D. Vollaro, 1990: External influence on hurricane intensity: Part II. Vertical structure and response of the hurricane vortex. *J. Atmos. Sci.*, **47,** 1902–1918.

NASA, 1979: Shuttle atmospheric lidar research program. Final report of Atmospheric Lidar Working Group SP-433, 220 pp.

——, 1982: Feasibility assessment: Satellite Doppler lidar wind measuring system. NASA Rep. MSFC-MOSD-146, 182 pp. [Available from NASA Marshall Space Flight Center, Huntsville, AL 35812.]

——, 1987: Laser atmospheric wind sounder. Earth observing system instrument panel report, Vol. IIg. Satellite Doppler lidar wind measuring system. NASA Rep. MSFC-MOSD-146, 55 pp.

Neiman, P. J., M. A. Shapiro, R. M. Hardesty, B. Boba Stankov, T. R. Lawrence, R. J. Zamora, and T. Hampel, 1988: The pulsed coherent Doppler lidar: Observations of front structure and the planetary boundary layer. *Mon. Wea. Rev.*, **116,** 1671–1681.

Penner, J. E., R. E. Dickinson, and C. A. O'Neill, 1992: Effects of aerosol from biomass burning on the global radiation budget. *Science,* **256,** 1432–1433.

Petterssen, S., and S. Smebye, 1971: On the development of extratropical cyclones. *Quart. J. Roy. Meteor. Soc.*, **9,** 457–485.

——, ——, D. L. Bradbury, and K. Pedersen, 1962: The Norwegian cyclone model in relation to heat and cold sources. *Geophys. Publ.*, **24,** 243–280.

Post, M. J., 1984a: Aerosol backscattering profiles at CO_2 wavelengths: The NOAA database. *Appl. Opt.*, **23,** 2507–2509.

——, 1984b: Lidar observations of the El Chichon cloud at lambda = 10.6 micrometers. *Geophys. Res. Lett.*, **1,** 846–849.

——, 1986: Atmospheric purging of El Chichon debris. *J. Geophys. Res.*, **91,** 5222–5228.

——, and R. E. Cupp, 1990: Optimizing a pulsed Doppler lidar. *Appl. Opt.*, **29,** 4145–4158.

——, and ——, 1992: CO_2 lidar backscatter profiles over Hawaii during fall 1988. *Appl. Opt.*, **31,** 4590–4599.

Randall, D. A., and Coauthors, 1992: Intercomparison and interpretation of surface energy fluxes in atmospheric general circulation models. *J. Geophys. Res.*, **97,** D4, 3711–3734.

Reed, R. J., and M. D. Albright, 1986: A case study of explosive cyclogenesis in the eastern Pacific. *Mon. Wea. Rev.*, **114,** 2297–2319.

Rohaly, G. D., and T. N. Krishnamurti, 1993: An observing system simulation experiment for the Laser Atmospheric Wind Sounder (LAWS). *J. Appl. Meteor.*, **32,** 1453–1471.

Rothermel, J., D. A. Bowdle, J. M. Vaughan, and M. J. Post, 1989: Evidence of a tropospheric aerosol background backscatter mode. *Appl. Opt.*, **28,** 1040–1042.

Rye, B. J., and R. M. Hardesty, 1993: Cramer-Rao lower bound-limited Doppler estimation using discrimination. *Proc. Seventh*

Conf. on Coherent Laser Radar Applications and Technology, Paris, France, CNES, CNRS, ESA, 217–220.

Sheets, R. C., 1990: The National Hurricane Center—past, present, and future. *Wea. Forecasting,* **5,** 185–232.

Shukla, J., C. Nobre, and P. J. Sellers, 1990: Amazon deforestation and climate change. *Science,* **247,** 1322–1325.

Steele, H. M., P. Hamill, M. P. McCormick, and T. J. Swissler, 1983: The formation of polar stratospheric clouds. *J. Atmos. Sci.,* **40,** 2055–2067.

Steinberg, R., 1983: Airline flight planning—the weather connection. *Proc. Symp. on Commercial Aviation Energy Strategies.* Washington, DC, DOE/FAA.

Tans, P. P., I. Y. Fung, and T. Takahashi, 1990: Observational constraints on the global atmospheric CO_2 budget. *Science,* **247,** 1431–1438.

Targ, R., M. J. Kavaya, R. M. Huffaker, and R. L. Bowles, 1991: Coherent lidar airborne windshear sensor: Performance evaluation. *Appl. Opt.,* **30,** 2013–2026.

Wang, M., J. Paegle, and J. N. Paegle, 1992: The role of topographically bound jets for moisture fluxes over North and South America. *Proc. Sixth Conf. on Mountain Meteorology,* Portland, OR, Amer. Meteor. Soc., 1–5.

Werner, C., P. Flamant, F. Köpp, C. Loth, H. Herrmann, J. Wildenauer, A. Dolfi-Bouteyre, and G. Ancellet, 1989: WIND: An advanced wind infrared Doppler lidar for mesoscale meteorological studies. Phase O/A study report to DLR and CNRS, 242 pp.

Wood, S. A., G. D. Emmitt, M. Morris, L. Wood, and D. Bai, 1993: Space-based Doppler lidar sampling strategies—Algorithm development and simulated observation experiments. Final report on NASA/Marshall Space Flight Center, Contract NAS8-38559, 226 pp. [Available from NASA/Marshall Space Flight Center, Huntsville, AL 35812.]

World Climate Research Program, 1986: Scientific plan for the World Ocean Circulation Experiment. WMO/TD-122, 83 pp.

Yue, G. K., G. S. Kent, U. O. Farrukh, and A. Deepak, 1983: Modeling atmospheric aerosol backscatter at CO_2 laser wavelengths. 3: Effects of changes in wavelength and ambient conditions. *Appl. Opt.,* **22,** 1671–1678.